ELSEVIER

Journal of Nuclear Materials 307–311 (2002) 293–298

journal of nuclear materials

www.elsevier.com/locate/jnucmat

Microstructural analysis of mechanically tested reduced-activation ferritic/martensitic steels

H. Tanigawa [a,*], T. Hirose [b], M. Ando [a], S. Jitsukawa [a], Y. Katoh [b], A. Kohyama [b]

[a] *Japan Atomic Energy Research Institute, 2-4 Shirakata-Shirane, Tokai-Mura, Ibaraki-ken 319-1195, Japan*
[b] *Institute of Advanced Energy, Kyoto University, Uji, Kyoto 611-0011, Japan*

Abstract

To make the best use of a limited number of irradiated strength-test specimens, it is desirable to derive the microstructure information related to the mechanical properties from mechanically tested specimens. A focused ion beam micro-sampling system was utilized to make thin film samples for transmission electron microscope (TEM) observations from the crack or fracture surface of the strength-tested specimens. The microstructure of mechanically tested specimens of a reduced-activation ferritic/martensitic steel, F82H, was investigated focusing on the irradiation effects on fatigue fracture. On unirradiated F82H, SEM observations revealed that the fatigue crack initiated along a prior austenite grain boundary. The TEM micrograph around the crack showed the presence of polygonization and the formation of distinctive shaped subgrains along the prior austenite grain boundary ahead of the crack. The fatigue crack initiated from an intergranular crack, and the TEM micrograph indicated that the main crack developed in the same manner as in the unirradiated F82H.

1. Introduction

It has been a key issue to gain understanding of the fracture process on a microstructural basis, especially in neutron-irradiated materials [1,2], but the process is not yet well understood because of the difficulty in making thin film samples from mechanically tested specimens for transmission electron microscope (TEM) observations. To solve this technical problem, a focused ion beam (FIB) micro-sampling system was installed in the Research Hot Laboratory of Japan Atomic Research Institute (JAERI), Japan. This system makes it possible to fabricate TEM specimens from the critical points of mechanically tested radioactive specimens, such as the crack initiation points in fatigue fracture in neutron irradiated specimens.

Fatigue properties of irradiated reduced-activation ferritic/martensitic steels (RAFs) are recognized as one of the important issues for fusion applications, especially for an ITER blanket module, because cyclic stress would be induced by ITER operation along with high-energy neutron irradiation and embrittlement by transmutant gas. For the moment, post-irradiation fatigue tests are useful to gain basic information on radiation damage effects on fatigue behavior of materials.

In case of post-irradiation mechanical tests, small specimen test techniques (SSTT) are very important because of the limitations in irradiation volume and the levels of radioactivity of irradiated specimens [3–5]. Because of the limitation in volume, it is difficult to irradiate enough specimens for each test condition. To evaluate the mechanical properties appropriately from these limited number of results, coupling of SSTT for post-irradiation strength tests and FIB micro-sampling technique for microstructural examination on fractured specimen could play an important role.

* Corresponding author. Tel.: +81-29 282 5391/6498; fax: +81-29 282 5922/5551.
E-mail addresses: tanigawa@realab01.tokai.jaeri.go.jp, tanigawa@popsvr.tokai.jaeri.go.jp (H. Tanigawa).

0022-3115/02/$ - see front matter
PII: S0022-3115(02)01002-4

Table 1
Chemical composition of F82H-IEA (mass %)

Fe	C	Si	Mn	P	S	Cr	Ni
Balance	0.09	0.07	0.1	0.003	0.001	7.87	0.02
Mo	V	Nb	N	Co	Ti	Ta	W
0.0003	0.19	0.0002	0.006	0.003	0.004	0.04	1.99

In this paper, the microstructure of fatigue-tested RAF specimens was investigated focusing on the irradiation effects on fatigue fracture.

2. Experimental procedure

The material used was Japanese RAF, F82H IEA heat [6]. The chemical composition of this steel is presented in Table 1. This steel was normalized at 1313 K for 30 min, and then tempered at 1013 K for 2 h.

Neutron irradiations up to a fluence of 3×10^{19} N/cm^2 ($E > 1.0$ MeV; about 0.02 dpa) at temperatures below 363 K were carried out on SF-1 miniaturized hourglass-shaped fatigue specimens [4,7] in the Japan Materials Testing Reactor (JMTR) at JAERI. Diametral strain-controlled low-cycle fatigue tests were carried out at ambient temperature with a total diametral strain range, $\Delta\varepsilon_t$, 1.0–2.0%. Following detailed observation of the fractured specimens with scanning electron microscopy (SEM), TEM specimens were fabricated from the regions beneath the points of initial crack and the fractured surface. The detailed procedures for fatigue tests and TEM specimen fabrication are presented elsewhere [8].

3. Results and discussions

3.1. Fatigue properties

Fig. 1 shows plastic strain range changes during fatigue tests on unirradiated and neutron-irradiated F82H. In all conditions, comparing those results obtained from the same diametral strain range tests, it is clear that plastic strain ranges in irradiated specimens are smaller than those of unirradiated specimens. This corresponds to hardening caused by low-temperature irradiation. Fig. 2 shows the fatigue lifetimes (N_f) of as-prepared and irradiated F82H. In general, the N_f of an irradiated specimen was shorter than that of the unirradiated one. In the case of $\Delta\varepsilon_t = 2\%$, the N_f was reduced to less than 10% of the unirradiated one. On the irradiated specimen tested at $\Delta\varepsilon_t = 1\%$, N_f is about 1.9×10^3, and this value itself is about the same as that of the unirradiated specimen tested at $\Delta\varepsilon_t = 1.5\%$, for

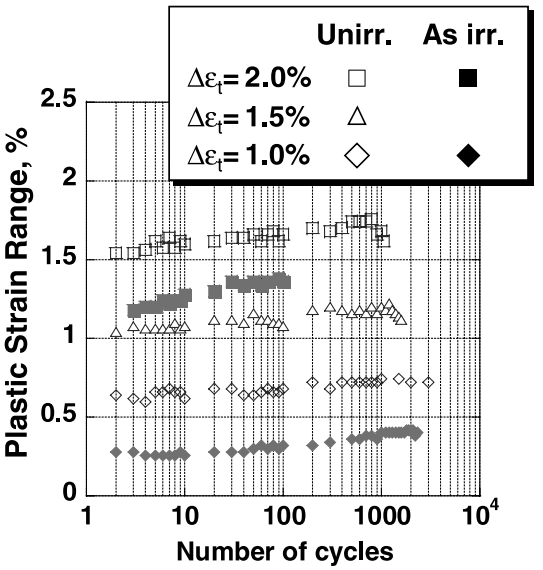

Fig. 1. Change in plastic strain range during fatigue tests.

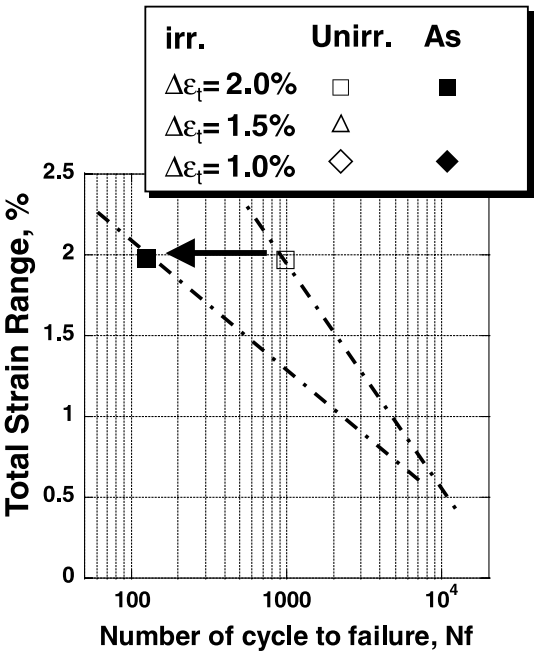

Fig. 2. Fatigue life in each condition.

which N_f is about 2.3×10^3. In the following sections, the fatigue fracture mechanisms corresponding to these two results will be discussed on a microstructural basis. The detailed discussion on a mechanical data basis is presented in an other paper [9].

3.2. SEM observations

SEM micrographs of the fracture surface on the unirradiated specimen are shown in Fig. 3. From these micrographs, it is seen that the fracture started from the

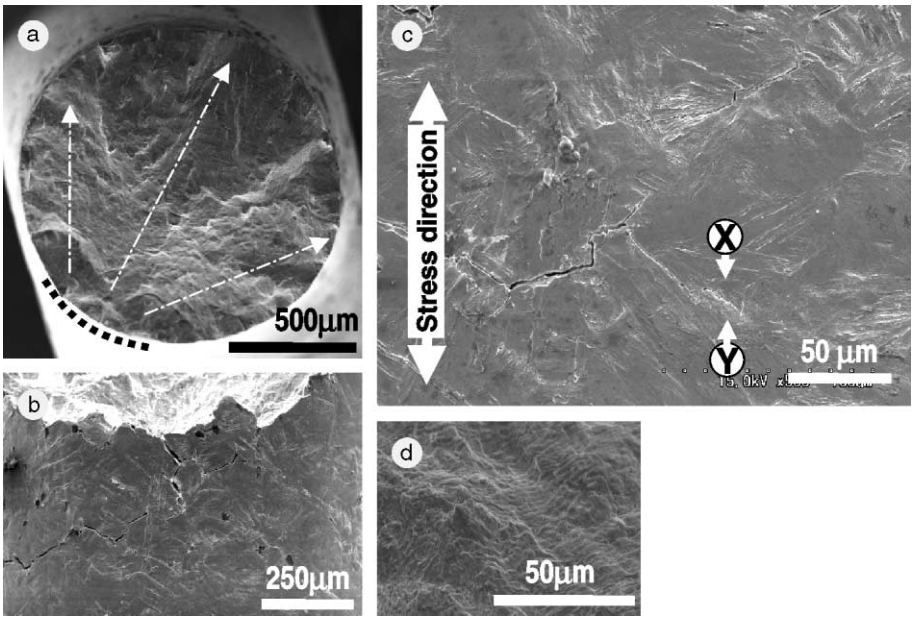

Fig. 3. SEM micrographs of fatigue fracture surface of unirradiated specimen: (a) top view, (b) side view of dotted line on (a), (c) magnified view of (b) with the region between denotation x and y, where TEM cross-sectional thin film was made from.

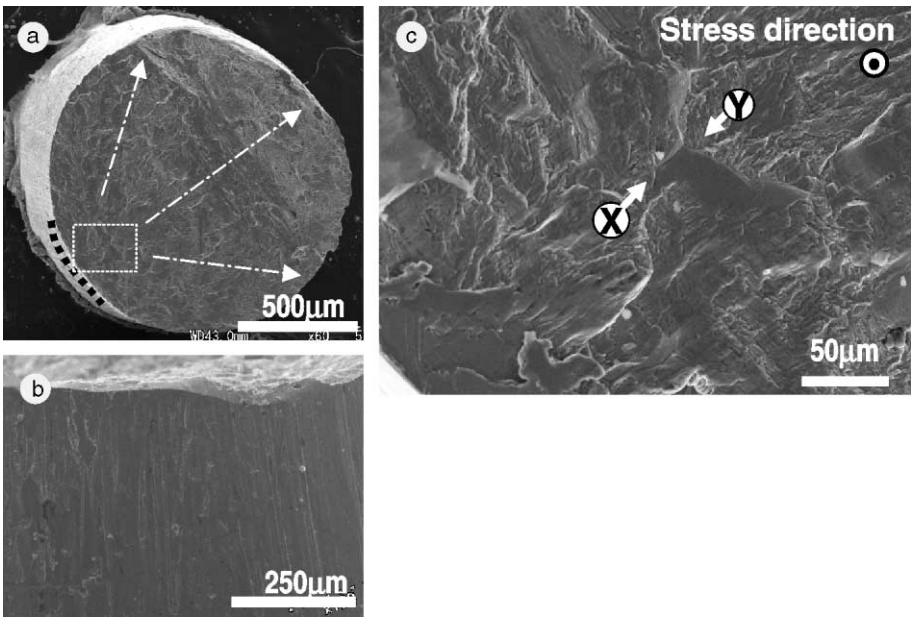

Fig. 4. SEM micrographs of fatigue fracture surface of irradiated specimen: (a) top view, (b) side view of dotted line on (a), (c) magnified view of dotted box on (c) with the region between denotation x and y, where TEM cross-sectional thin film was made from.

side denoted by the dotted line on the micrograph (a), and this crack penetrated in the direction denoted by the white dashed arrow on this specimen. This fracture surface was inclined at 45° to the stress axis. Lots of cracks were observed on the side where the fracture started (Fig. 3(b)), and they propagated along prior austenitic grain boundaries (Fig. 3(c)). Although the fracture might have started in a brittle manner as this, the observed striation pattern suggests that the main crack penetrated in a ductile manner (Fig. 3(d)) [10].

In the irradiated specimen, where the main crack propagation direction is denoted in the same manner on Fig. 4(a), the fatigue fracture proceeded in a totally ductile manner. No obvious cracks were observed on the side of the specimen, as it was covered with mechanical polishing scratches (Fig. 4(b)). As shown in Fig. 4(c), an intergranular fracture surface was observed in the middle of the area that was denoted by the white dashed box on Fig. 4(a). This point could be the starting point of the fracture, because all fracture patterns converged to this point.

3.3. TEM observations

Fig. 5 shows the microstructure of the cross-sectional region around a crack tip. This was observed on the side of the specimen where the fracture started, which is shown by the schematic drawing. The exact point where the thin film sample was made is shown in Fig. 3(c), the region between points denoted by x and y. In Fig. 6, microstructures of (a) an as-prepared specimen and (b) a 20 cycle fatigue-tested specimen are shown for comparison. These results show that F82H has the typical RAFs

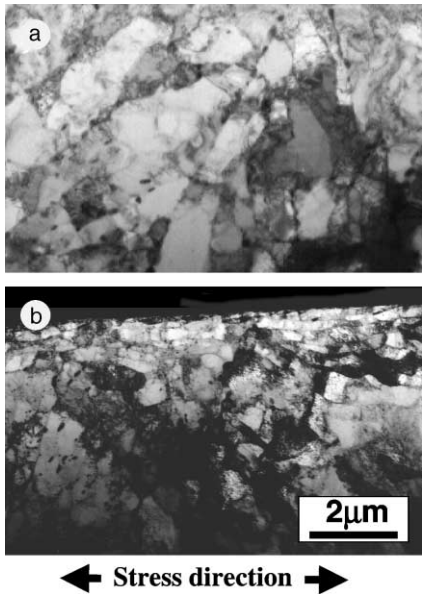

Fig. 6. TEM micrographs of (a) as prepared F82H, and (b) 20 cycle fatigue-tested F82H.

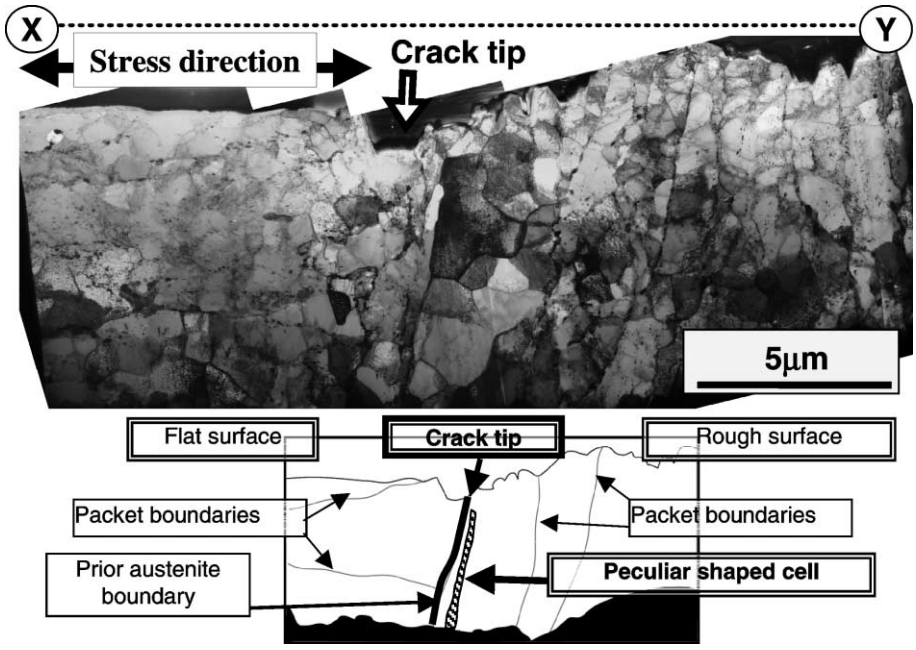

Fig. 5. TEM micrograph and its schematic illustration of fatigue crack tip of unirradiated F82H. The sampled region was shown in Fig. 3(c). Stress axis was on the TEM thin film.

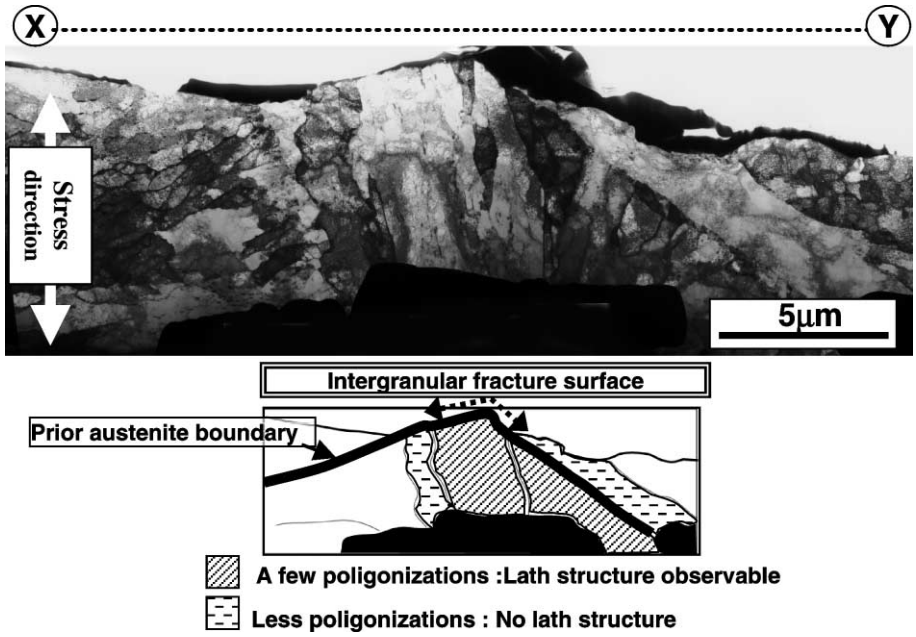

Fig. 7. TEM micrograph and its schematic illustration of fatigue fracture surface of irradiated F82H. The sampled region was shown in Fig. 4(c). Stress axis was on the TEM thin film.

microstructure with a lath structure before testing (Fig. 6(a)). However, the lath structure vanished and polygonization [11,12] was observed by at 20 cycles of fatigue (Fig. 6(b)), and this results in the formation of cell structures (subgrains), as shown in Fig. 5. A peculiar-shaped subgrain was observed beneath the crack tip, along with a prior austenite grain boundary (Fig. 5). As this subgrain was penetrating pre-formed subgrains, it appears to be formed in the last stage of the fracture process. No typical fatigue microstructures, such as a vein structure or persistent slip bands [13,14] were observed.

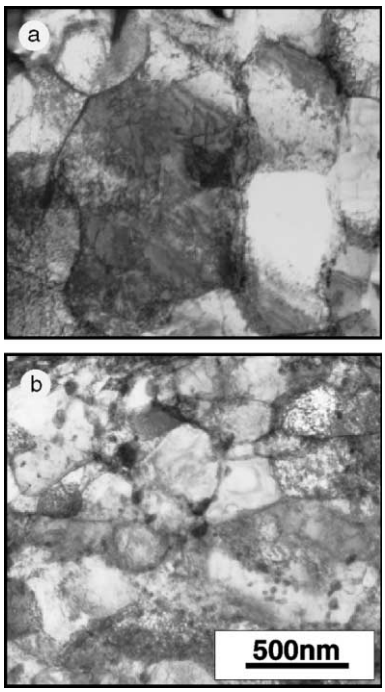

Fig. 8. TEM micrographs of cell structures observed in (a) unirradiated and (b) irradiated F82H.

Fig. 7 shows microstructures of the cross-sectional region beneath points x and y shown in Fig. 4(c), along with the schematic drawing of the microstructure. Cell structures were also observed as in the unirradiated specimen. Subgrain sizes were smaller than that of the unirradiated specimen (Fig. 8), and this can be correlated to the difference in plastic strain range. It should be noted that the microstructure beneath the intergranular fracture region (Fig. 7) shows a less polygonized structure. This implies that intergranular fracture occurred in the early stage of fatigue.

4. Mechanisms of fatigue fracture

From these results, mechanisms of the fatigue fracture process based on microstructure changes are suggested.

In the unirradiated specimen: (a) lath structures vanished and polygonization occurred in the early stage

of fatigue, (b) polygonization proceeded and subgrain structures were formed gradually, and then (c) a peculiar shaped subgrain was newly formed along a prior austenite grain boundary, and the crack was initiated at the portion of prior austenite grain boundary open to the surface, and at last (d) the crack penetrated through the specimen forming the striation pattern.

In the irradiated specimen: (A) intergranular fracture occurred with no relation to the polygonization process, then (B) polygonization occurred in the early stage of fatigue, where the size of the polygons become small relative to the strain range, and (C) the crack propagates slowly compared to the unirradiated specimen, relative to the plastic strain range, then (D) the crack propagates along a or nearby weakest region, such as a portion of a prior austenite grain boundary.

5. Summary

The microstructure of fatigue-tested specimens of RAF was investigated with emphasis on the fatigue fracture mechanism and on the effect of irradiation thereon. The following conclusions were reached:

(1) Alternating strain destroys the lath structure and induces polygonization.
(2) Irradiation hardening causes a decrease in the strain range, and a size reduction of polygonized regions.
(3) Crack initiation occurs as the final phase of polygonization in the unirradiated specimen, but it occured earlier in fatigue for the irradiated specimen, perhaps because the grain boundary becomes brittle by irradiation.

Acknowledgements

The authors are grateful to staff of Oarai branch, Institute for Material Research, Tohoku University for utilizing hot laboratories.

References

[1] G.E. Lucas, D.S. Gelles, J. Nucl. Mater. 155–157 (1988) 164.
[2] G.R. Odette, J. Nucl. Mater. 212–215 (1994) 45.
[3] P. Jung, H. Ullmaier (Eds.), Miniaturized Specimens for Testing of Irradiated Materials, Forschungszentrum Jülich, Jülich, Germany, 1995.
[4] Y. Miwa, S. Jitsukawa, A. Hishinuma, J. Nucl. Mater. 258–263 (1998) 457.
[5] J. Bertsch, S. Meyer, A. Möslang, J. Nucl. Mater. 283–287 (2000) 832.
[6] T. Ishii, K. Fukaya, Y. Nishiyama, M. Suzuki, M. Eto, J. Nucl. Mater. 258–263 (1998) 1183.
[7] T. Hirose, H. Tanigawa, M. Ando, T. Suzuki, A. Kohyama, Y. Katoh, M. Narui, in: M.A. Sokolov, J.D. Landes, G.E. Lucas (Eds.), Small Specimen Test Techniques: Fourth Volume, ASTM STP 1418, American Society for Testing and Materials, West Conshohocken, PA, 2002.
[8] T. Hirose, H. Tanigawa, M. Ando, A. Kohyama, Mater. Trans. 43 (2001) 389.
[9] T. Hirose, H. Tanigawa, M. Ando, A. Kohyama, Y. Katoh, M. Narui, these Proceedings.
[10] R.W. Hertzberg, in: Deformation and Fracture Mechanics of Engineering Materials, 4th Ed., John Wiley, New York, 1996, p. 606.
[11] H.J. Chang, J.J. Kai, J. Nucl. Mater. 191–194 (1992) 836.
[12] T. Yokoi, M. Takahashi, N. Maruyama, M. Sugiyama, J. Mater. Sci. 36 (2001) 5757.
[13] T. Tabata, H. Fujita, M. Hiraoka, K. Onishi, Philos. Mag. A 47 (1983) 841.
[14] O.B. Pedersen, A.T. Winter, Phys. Stat. Sol. (a) 149 (1995) 281.